

University of Nebraska - Lincoln

DigitalCommons@University of Nebraska - Lincoln

Faculty Publications, Department of Physics
and Astronomy

Research Papers in Physics and Astronomy

4-3-2023

A Method to Measure Positron Beam Polarization Using Optically Polarized Atoms

Joshua Joshua Machacek

Sean Hodgman

Stephen Buckman

T. J. Gay

Follow this and additional works at: <https://digitalcommons.unl.edu/physicsfacpub>




Part of the [Physics Commons](#)

This Article is brought to you for free and open access by the Research Papers in Physics and Astronomy at DigitalCommons@University of Nebraska - Lincoln. It has been accepted for inclusion in Faculty Publications, Department of Physics and Astronomy by an authorized administrator of DigitalCommons@University of Nebraska - Lincoln.

Article

A Method to Measure Positron Beam Polarization Using Optically Polarized Atoms

Joshua R. Machacek ¹, Sean Hodgman ¹, Stephen Buckman ^{1,2,*} and T. J. Gay ³ 

¹ Research School of Physics, Australian National University, Canberra, ACT 2601, Australia; joshua.machacek@anu.edu.au (J.R.M.); sean.hodgman@anu.edu.au (S.H.)

² Department of Actuarial Science and Applied Statistics, Faculty of Business and Information Science, UCSI University, Kuala Lumpur 56000, Malaysia

³ Center for Materials and Nanoscience, Jorgensen Hall, University of Nebraska, Lincoln, NE 68588, USA; tgay@unl.edu

* Correspondence: stephen.buckman@anu.edu.au

Abstract: We outline an experimental technique for measuring the degree of polarization of a positron beam using an optically pumped, spin-polarized Rb target. The technique is based on the production and measurement of the ortho- and para-positronium fractions through positron collisions with the Rb atoms as a function of their polarization. Using realistic estimates for the cross sections and experimental parameters involved, we estimate that a polarization measurement with an uncertainty of 3% of the measured value can be achieved in an hour.

Keywords: positron; positronium; polarization; optical pumping; helicity

1. Introduction

The interest in polarized positron beams, together with a knowledge of the beam polarization, has been driven by a number of realised or potential applications of positron and positronium (Ps) science. These include the study of surfaces and magnetic materials via a range of positron spectroscopies (PALS—Positron Annihilation Lifetime Spectroscopy; ACAR—Angular Correlation of Annihilation Radiation; DBS—Doppler Broadening Spectroscopy) [1], potential applications in spintronics [1,2], and spin-polarized positron-induced Ps spectroscopy for probing the spin-dependent surface density of states [3]. Most exciting is the prospect of the creation of a positronium Bose–Einstein condensate through the creation of a high density, spin-polarized Ps ‘gas’, (see, e.g., [4–7]). To this end, positron polarimetry has been developed extensively since the violation of parity conservation in the weak interactions was first discovered [8]. Improvements in polarimetry enable development and testing of new source configurations to produce highly polarized positron beams and for the measurement of spin-dependent scattering processes. We discuss here the concept of using an optically pumped target as a polarimeter as compared to previous polarimetry designs.

The most commonly used positron source is based on the nuclear beta decay of radioactive isotopes, and amongst these, ²²Na is a laboratory favourite due to its relatively long half-life of 2.6 years and 90% conversion rate for positron production. Positrons produced in ²²Na decay have energies of between 0 and 546 keV with an average energy of 216 keV [9]. As a result of parity non-conservation in the beta decay process, the emitted positrons are longitudinally spin-polarized, with their degree of polarization given by Cv/c , where v is the emission velocity, c is the speed of light, and C is a constant that is near or equal to unity for most beta decay processes. At a mean emission energy of ~200 keV for ²²Na, the polarization along the emission direction is thus about 70% [10].

To form a positron beam of reasonably narrow energy width that can be used for atomic collision physics experiments, it is necessary to “moderate” (slow down) the emitted positrons. However, the nature of the positron source configuration, the range of



Citation: Machacek, J.R.; Hodgman, S.; Buckman, S.; Gay, T.J. A Method to Measure Positron Beam Polarization Using Optically Polarized Atoms. *Atoms* **2023**, *11*, 65. <https://doi.org/10.3390/atoms11040065>

Academic Editor: Sabyasachi Kar

Received: 28 February 2023

Revised: 21 March 2023

Accepted: 22 March 2023

Published: 3 April 2023



Copyright: © 2023 by the authors. Licensee MDPI, Basel, Switzerland. This article is an open access article distributed under the terms and conditions of the Creative Commons Attribution (CC BY) license (<https://creativecommons.org/licenses/by/4.0/>).

emission angles that are captured in the beam, the moderation process itself, and a host of beam-transport mechanisms can alter the nascent positron polarization. A thorough characterization of the experiment in which the positrons are ultimately used generally requires that the positron beam polarization, P_{e^+} , be known [11]. The value of P_{e^+} can be defined as:

$$P_{e^+} = \frac{N^+ - N^-}{N^+ + N^-},$$

where $N^{+(-)}$ is the number of e^+ with spin up (down) along a specified axis, which is most typically the axis parallel to the positron beam’s momentum.

Polarimeters based on Mott scattering are not generally practicable; the repulsive Coulomb force between positrons and high-Z nuclei minimises the spin-orbit coupling that yields the necessary spatial spin asymmetry required for polarimetric analysis. The analysing power of positron scattering from, e.g., Hg targets is roughly one-tenth of that for electrons below 200 keV and is essentially zero below 50 keV, corresponding to a deficit in statistical accuracy of two orders of magnitude for a given counting time and beam current [12]. Even at energies above 1 MeV, the positron analysing power is only about half that for electrons. Positron polarimeters based on Bhabba scattering have been built and have reasonable analysing power above 1 MeV [13], but, again, they are not suitable for analysing positron beams in the keV (or lower) energy range.

The majority of positron polarimeters discussed in the literature are not based on two-body scattering, but on the formation of positronium through positron scattering from a target in a strong magnetic field, and the subsequent coincidence rate measurements of either the back-to-back two-gamma (2γ) emission from para-positronium (p -Ps) decay, or the time-delayed 3γ decay of ortho-positronium (o -Ps) [8,11,14]. When a beam of polarized positrons strikes a target with electron polarization

$$P_T = \frac{N_T^+ - N_T^-}{N_T^+ + N_T^-}$$

where, as before, $N_T^{+(-)}$ is the number of electrons with $+(-)$ spin along a specified axis, one can show that, in the absence of spin-orbit-induced spin flips, and in the limit of no magnetic mixing of p -Ps and o -Ps, the probability of producing o -Ps and p -Ps depends on P_T and P_{e^+} as indicated in Table 1.

Table 1. Relative production probabilities of ortho-positronium (o -Ps) and para-positronium (p -Ps) for a target of electron polarization P_T and a positron beam of polarization P_{e^+} .

Target Spin	Beam Spin	Configuration Probability	Relative o -Ps Production	Relative p -Ps Production
+	+	$1/4 (1 + P_{e^+} + P_T + P_{e^+} P_T)$	1	0
+	−	$1/4 (1 - P_{e^+} + P_T - P_{e^+} P_T)$	1/2	1/2
−	+	$1/4 (1 + P_{e^+} - P_T - P_{e^+} P_T)$	1/2	1/2
−	−	$1/4 (1 - P_{e^+} - P_T + P_{e^+} P_T)$	1	0

The first example of positron polarimetry based on positronium formation was demonstrated in 1957 by Hanna and Preston [8,15]. In their experiment, polarized positrons from ^{64}Cu beta decay formed positronium as the result of being stopped in a magnetized iron target. The 2γ coincidence rate was measured as a function of the target magnetization direction, either parallel or anti-parallel to the positron beam axis. Since (except at very high magnetic fields) the 2γ rate is due almost exclusively to the formation of p -Ps, it is apparent from Table 1 that this rate will change when the iron magnetization (and hence, P_T), is flipped. The change in coincidence rate can thus be used to extract P_{e^+} . The experiment of Hanna and Preston, while pioneering the field of positronium-based polarimetry, was plagued by small spin asymmetries due to the low values of P_T in the magnetized iron.

It also relied on magnetic field flipping to obtain these asymmetries, which is relatively slow and can cause instrumental asymmetries in the measurement. An improved version of such a polarimeter has been described more recently by Nagashima and Hyodo [16].

Independently, Page and Heinberg [17] showed that a magnetized target could be replaced by unpolarized gas. A magnetic field of ~ 1 T was used, not to spin polarize the gas, but to mix the singlet and triplet ($m = 0$) states of the positronium so that their Zeeman-perturbed states would exhibit a 2γ coincidence rate that depended on the magnetic field magnitude and direction as well as P_{e^+} .

A significant improvement over these techniques was subsequently proposed independently by Telegdi [18] and Lundby [19], demonstrated by Dick et al. [20] and Bisi et al. [21], and improved further and used extensively by Rich and co-workers [22–24] and Kumita et al. [25]. This method also employs a strong (~ 1 T) field to mix the singlet and triplet states, but is based on coincidence events in time, as opposed to angle. In the prototype experiment of Gerber et al. [22], incident positrons from a ^{68}Ga source, embedded in a field of ± 0.29 T, formed positronium in a MgO powder target. Prior to entering the MgO target, the positrons traversed a thin scintillator which provided the start signal for a timing measurement. Subsequent decay of the $m = 0$ magnetically perturbed o -Ps occurred with a lifetime close to its unperturbed value—about 142 ns. By looking at coincidence events separated by more than this lifetime after the start pulse, the p -Ps decays were effectively eliminated. An asymmetry constructed from the coincidence rates measured for the “forward” and “backward” magnetic field directions yielded P_{e^+} .

More recently, the UC Riverside group has developed a novel polarimetric method in which the incident positrons, whose polarization is to be determined, form Ps in the solid regions of a porous silica film in a high magnetic field [26]. The Ps atoms can subsequently diffuse into the silica voids. Para-Ps states, which can be made directly by electron capture, magnetic-field quenching, or in exchange collisions between two o -Ps atoms in opposite $m = \pm 1$ states, decay quickly. When all of the o -Ps associated with the minority spins of the incident polarized positron beam have been quenched in collisions with o -Ps associated with the majority spins, the remaining fraction of delayed decays (between 50 ns to 300 ns after the incident positron pulse enters the silica target) gives the incident P_{e^+} . This remaining fraction of o -Ps is also completely polarized, making it suitable, at least in principle, for the formation of a Ps Bose–Einstein condensate.

We are interested in studying collisions between positrons and a variety of atoms and molecules. The positrons are produced using a ^{22}Na source, moderated with solid neon, and accumulated and cooled in a Surko buffer gas trap (BGT) [27]. With a nominal 50 mCi ^{22}Na source, the trap produces pulses of about 2×10^6 positrons and 20 ns duration at repetition rates between 1 and 10 Hz depending on operational conditions and the energy resolution required. As a general tool for monitoring our positron beamline, we plan to use a novel positron polarimetric method that we propose here. It has the advantages of simplicity, high analysing power, and optical spin reversibility of the target electron polarization, without the need of a high (~ 1 T) magnetic field. The latter feature can be important if, e.g., the polarimeter is to be placed near a target chamber that must be kept at very low magnetic field.

2. Method

We propose to use as a polarimetric target optically pumped Rb, with a spin polarization $P_{Rb} \equiv P_T$. In such a scheme, a circularly polarized (σ^+) laser with enough power to saturate the Rb D1 transition at 795 nm traverses a Rb vapor target in a direction parallel to a weak (< 0.02 T) applied magnetic field (Figure 1). Through repeated cycles of absorption and emission of the D1 light, the ground-state Rb atoms become spin-polarized. Emission of linearly-polarized light from the Rb excited state can depolarize the sample due to radiation trapping unless (a), the density of Rb is low so that the reabsorption probability is low, (b) the magnetic field is high enough that the Rb atoms are in the Paschen–Back regime,

or (c), a buffer gas such as N₂ is added to quench the excited states without spin-flip before they can fluoresce [28–31].

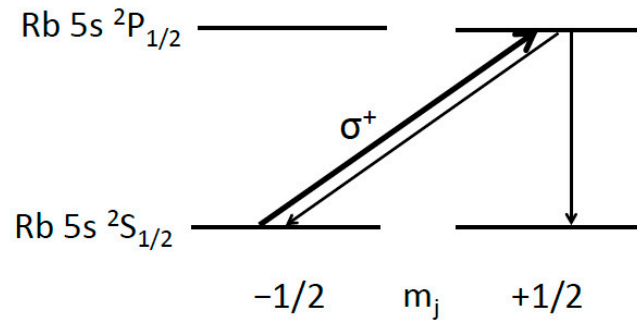


Figure 1. Schematic diagram of Rb optical pumping with circularly polarized (σ^+) D1 795 nm laser light. Repeated cycles of absorption, emission, and reabsorption produce ground-state Rb that is highly spin polarized. Atoms in the $m_j = +1/2$ “dark” ground state cannot absorb a σ^+ photon.

We would restrict the Rb number density to $\sim 10^{11} \text{ cm}^{-3}$ to obviate the need for a buffer gas [28,29], and restrict the target’s transverse dimensions to $<1 \text{ cm}$ to minimize the effects of radiation trapping and allow P_T in excess of 90% [30,31]. The value of P_T can be determined in situ by means of optical rotation measurements of a weak probe laser that does not affect the optical pumping process [32]. In the simplest scenario, polarized positrons will capture the polarized Rb valence electrons and form *o*-Ps and *p*-Ps in the ratios given in Table 1. In the magnetic fields used for low-density Rb optical pumping ($\sim 10^{-2} \text{ T}$), positronium produced in the spin-triplet ground state (3S_1 ; *o*-Ps) decays almost exclusively by 3γ decay with a lifetime of 142 ns. Ps produced in the spin-singlet ground state (1S_0 ; *p*-Ps), decays into two gammas with a lifetime of 125 ps [8,11]. Using a photomultiplier tube (PMT) and scintillator (e.g., NaI) to monitor the Rb charge transfer target cell, we would detect only Ps decay events that occur more than 100 ns after a positron pulse has reached the Rb target, as determined by a 20-ns-duration start signal caused by prompt decay of *p*-Ps. The various singlet and triplet states will have essentially the relative populations given in Table 1. Thus, for N incident positrons, and assuming that the probability for any given positron to capture an electron (e.g., direct annihilation) is $\ll 1$, the number of *o*-Ps atoms produced is

$$N_o = \frac{1}{4} N \sigma n l [3 + P_B P_T],$$

where σ is the Ps formation cross section, n is the density of Rb in the collision volume, and l is the effective path length in the optically pumped Rb. Similarly, for *p*-Ps,

$$N_p = \frac{1}{4} N \sigma n l [3 - P_B P_T].$$

Upon flipping the helicity of the optical pumping laser light, the sign of P_T flips as well. By waiting long enough to eliminate any prompt annihilation signal and for the *p*-Ps to completely decay, we can construct a polarimetric asymmetry by reversing the pump helicity:

$$A = \frac{R^+ - R^-}{R^+ + R^-} = \frac{1}{3} P_B P_T.$$

3. Proposed Apparatus

A proposed prototype polarimeter is shown schematically in Figure 2. The entire apparatus is immersed in an axial B-field of about 10^{-2} T , produced by solenoidal coils. This field would be joined smoothly, to ensure adiabatic transport [33], with the B-fields used for trapping and transporting the positron beam from the BGT to the polarimeter and any subsequent downstream targets. Upon leaving the BGT, the positron beam traverses a

differential pumping region defined by two apertures that serve to improve the vacuum isolation of the Rb polarimeter target. A fast TTL signal is provided by the BGT which acts as a start signal described above.

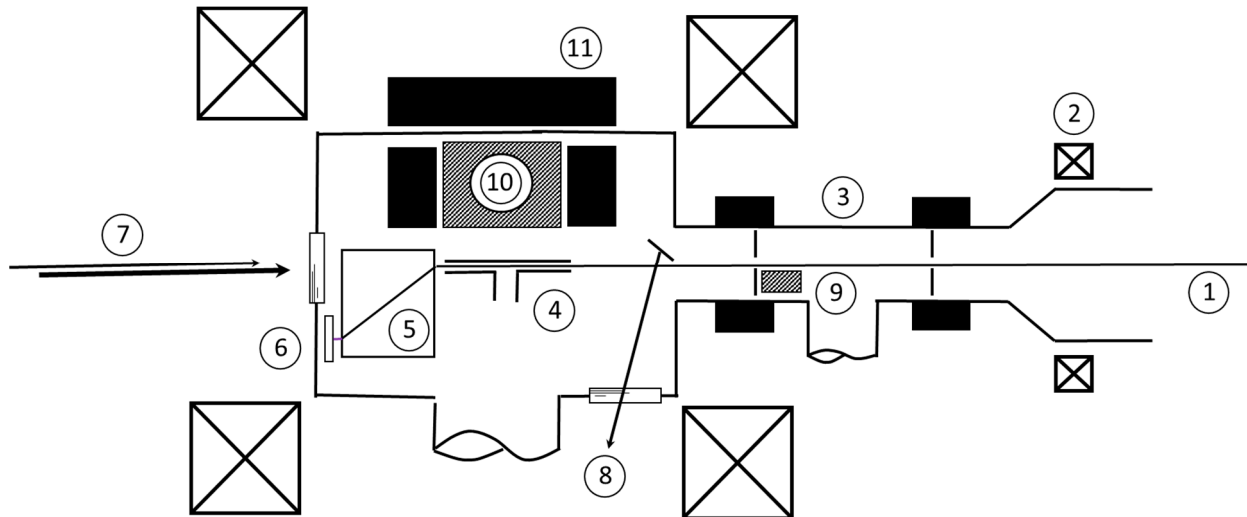


Figure 2. Schematic diagram of the positron polarimeter showing (1) terminus of the Surko buffer gas trap and incident positron beam guided by (2) solenoidal magnets; (3) differential pumping section; (4) the heated, optically pumped Rb target; (5) trochoidal beam deflector that directs the positrons to a beam dump (6); (7) optical pumping and probe lasers; 980 reflected probe beam to monitor Rb polarization; (8) reflected probe beam used to measure Rb polarization; (9) (NaI) scintillators (cross-hatched regions) that provide the event detection; (10) the target photomultiplier tube, and (11) Pb blocks to keep stray gamma rays from striking the scintillators.

The BGT employs a rotating wall technique [34] to compress the positron cloud, trapped longitudinally in a harmonic potential, in the radial direction to approximately 1 mm in diameter at a BGT field of ~ 0.05 T. Heating due to the RF drive is removed by a sufficient density of cooling gas, in this case CF_4 , allowing the positron ensemble to thermalize with the room-temperature system [35].

The polarimeter target system comprises a Rb reservoir and a heat pipe of narrow transverse dimension to suppress Rb depolarization due to optical trapping [30,31]. The optical pumping laser should have several watts of power at the Rb D1 transition ($5s^2S_{1/2}-5p^2P^o_{1/2}$) frequency and a variable width of ~ 0.6 GHz [29]. A single-mode low-power (<1 mW) polarimetric probe laser at the Rb D2 transition ($5s^2S_{1/2}-5p^2P^o_{3/2}$) frequency would also traverse the heat pipe and be used to measure P_T , providing in situ calibration of the polarimeter's analysing power [36]. (We note that this is similar to the calibration scheme for electron Mott polarimetry involving optical pumping of metastable He developed by the Rice group [37].) Upon exiting the charge-transfer cell, the positron beam is shunted to a beam dump by a transverse trochoidal electric field deflector [38]. This beam dump must be positioned sufficiently far from the polarimeter collision region to ensure Ps atoms formed at the beam dump do not enter the field of view of the scintillator.

Directly above the Rb heat pipe, a (NaI) scintillator block would monitor annihilation gammas, timed to occur more than 100 ns after the positron pulse from the BGT has reached the target. This delay will eliminate all of the prompt annihilation background signal produced by p -Ps decay or direct annihilation in collisions of positrons or positronium with the heat pipe walls. We anticipate that the primary scintillator can subtend a solid angle of one steradian about a point on the beamline within the Rb target. This scintillator would be well shielded on its top and sides to minimize background due to cosmic rays and beam-related annihilation events occurring well outside the Rb target.

The choice of a NaI scintillator is based upon its high efficiency rather than timing performance [39]. It is worth noting that for a sufficiently high number of positrons in a temporally compressed beam, saturation can occur. Thus, less efficient but faster scintillators could be used (e.g., liquid [40] or LYSO [41]). This is a trade-off between detection efficiency and the time response of the scintillator, with faster scintillators allowing a more detailed investigation of the positron lifetime (e.g., using Ps time-of-flight).

4. Collisional Considerations

We now consider in detail the Rb collisional processes relevant to the proposed polarimeter. The vast majority of the optically pumped atoms at the Rb density we consider will be in the dark ground state. The target cell is best held at a voltage that causes the positrons to have a kinetic energy that optimizes the charge transfer cross section for positronium production, while at the same time minimizing the deleterious effects of other collision channels. The kinetic energy of the positron beam can be set by adjusting the potential of the Rb charge transfer target cell with respect to the positron beam potential set by the last electrode of the BGT; this is straightforward for a longitudinal beamline magnetic field of 10^{-2} Tesla. In the following discussion, we assume a Rb density $n_{Rb} = 10^{11} \text{ cm}^{-3}$, and a length of the Rb heat pipe equal to 3 cm.

The threshold for positronium formation from an atom or molecule with ionization potential I is $eI = 6.8 \text{ eV}$. Thus, formation of positronium by charge transfer from Rb can occur for any incident positron energy, since $I_{Rb} = 4.2 \text{ eV}$. Direct annihilation of the incident e^+ by Rb in “pick-off” collisions, open at all collisional energies, is highly unlikely given that the pick-off cross section is much smaller than that for Ps formation and would lead only to a low-level prompt background that we discriminate against [11,14]. Thus, we need only consider Ps-forming charge-transfer collisions, inelastic excitation and ionization, and elastic scattering.

Between 1 and 5 eV (where it peaks), the total positronium formation cross section σ_{Ps}^{tot} increases from about $10 \times 10^{-16} \text{ cm}^2$ to $40 \times 10^{-16} \text{ cm}^2$ [42]. The threshold for excitation of $n = 2$ Ps is at 2.5 eV, and the $n = 3$ threshold is 3.4 eV. We consider a positron energy of 2.4 eV, just below the Ps ($n = 2$) threshold, as this obviates any complications in the timing spectrum due to excited states [43]. This does not sacrifice a significant amount of Ps production rate but gives a clean signal from the Ps $n = 1$ triplet states following a 100 ns post-collision delay.

At 2.4 eV, the appreciable cross sections are an $n = 1$ Ps production cross section of about $25 \times 10^{-16} \text{ cm}^2$, a 5s-5p total excitation cross section of $20 \times 10^{-16} \text{ cm}^2$ [44], and a total scattering cross section of $100 \times 10^{-16} \text{ cm}^2$ [45]. This means that about five times as many positrons will scatter as produce Ps. These cross sections have been summarized and shown graphically in part 4.10 of [42].

5. Timing and Polarimetric Efficiency

The Surko BGT at the ANU produces positron pulses that are no more than a millimetre in diameter. The inner diameter of the spin-transfer heat pipe should be as small as possible to minimize radiation trapping depolarization of the Rb. According to the calculations of Tupa and Anderson [31], a heat pipe diameter of 5 mm is sufficiently narrow to effectively eliminate depolarization due to radiation trapping. Positrons that scatter from the Rb atoms, both elastically and inelastically, will be effectively kept away from the heat pipe walls by their cyclotron orbits in the 10^{-2} T ambient B field. In any case, the probability that they will directly annihilate on the Rb-coated walls of the heat pipe after a few collisions is very small [14]. Pick-off and exchange quenching of newly formed *o*-Ps is expected to be very small as well ([11], p. 328), but in any case, a quenching event would lead to annihilation gammas that would be prompt and that could thus be temporally excluded by the detection timing circuit.

We now calculate the rate of gammas produced greater than 100 ns after the positron bunch has traversed the Rb target. A minimal pulse of 2×10^6 positrons occurring at 1 Hz

will result in an *o*-Ps ($n = 1$) production rate of $1.1 \times 10^3 \text{ s}^{-1}$, assuming three-quarters of the $n = 1$ Ps are in the triplet state, with a production cross section of $25 \times 10^{-16} \text{ cm}^2$, and a Rb density of 10^{11} cm^{-3} . With an *o*-Ps annihilation lifetime of 140 ns, 49% of these will decay after 100 ns, and be counted as signal. Of these, about 10% will intercept the large scintillator, with a $\sim 100\%$ detection due to the combined conversion efficiency (38 visible photons/keV) of the scintillator and the quantum efficiency (>0.2 at 415 nm) of the photomultiplier tube. This corresponds to a count rate of 55 Hz. We can also characterize this technique with a “polarimetric figure of merit”, F [46]:

$$F = \frac{R}{R_0} A^2$$

where R and R_0 are the detected gamma and incident positron rates, respectively and A is the polarimetric analysing power. Thus, $F = 3 \times 10^{-6}$ and a positron beam having 22% polarization could have its polarization measured with a precision of 10% of its value in <6 min, or 3% in an hour. Unfortunately, F has not been calculated for previous positron polarimeters, so comparison is not possible. While the figures we have used may correspond to ideal circumstances with respect to positron flux, polarization fraction, and atomic number density, they are intended to demonstrate the broad feasibility of the proposed methodology.

6. Discussion

Positron polarimetry using a spin-polarized target is of general utility. While we have discussed polarized Rb as the target, this choice was motivated primarily because of the availability of lasers and the large amount of work done on the optical manipulation of Rb from room temperature to temperatures required for the production of Bose–Einstein condensates. Generally, any target ensemble whose spin-polarization can be flipped with respect to that of the positron beam can be used as a positron polarimeter. Some examples include other atomic or molecular gaseous targets with cyclable transitions, and condensed matter systems such as optically active defects. We also note that Monte Carlo simulations have been qualitatively successful in modelling spin-exchange between optically pumped Rb vapor targets and low-energy electron beams [47]. This is a process that has many similarities to the positron–Rb interactions we consider here.

Our proposal can be extended, in principle, to cold atom systems such as Rb in a magneto-optical trap (MOT). A Rb-MOT has the advantage of fine control of the quantization axis, temperature, and spatial distribution of the Rb cloud. The number of atoms in a Rb-MOT typically saturates at $\sim 10^8$ with current techniques enabling number densities up to 10^{12} cm^{-3} resulting in a Rb cloud of $\sim 0.2 \text{ mm}$ [48]. The current transverse spatial dimension of the positron beam we can produce is $\sim 1 \text{ mm}$, which can be improved by careful control of stray magnetic fields and other asymmetries in the BGT. An additional challenge in using a MOT is the guiding of the positron beam to the cold-atom target. The magnetic field gradient ($\sim 10^{-4} \text{ T/mm}$) used to tune the hyper-fine splitting of the neutral atoms in the MOT must be switched off before the strong field ($\sim 0.05 \text{ T}$) required to guide the positrons to the target is turned on. Fast switching of solenoidal coils has been demonstrated using custom circuits [49].

7. Conclusions

We have proposed a novel experimental technique to efficiently and accurately measure the degree of polarization of a beam of positrons from a beta-decay source. The technique requires a tightly compressed, pulsed, low-energy positron beam with a narrow energy distribution ($\sim 50 \text{ meV}$), as is obtained from a Surko buffer gas trap. This beam is incident on an optically pumped source of Rb atoms whose polarization can be readily varied by flipping the helicity of the pump laser. Using reasonable estimates of the important experimental parameters, we estimate that an accurate measurement of the beam polarization can be made in a time of the order of minutes. Such a knowledge of the beam

polarization would be useful in a number of applications of positron science, including studies of magnetic materials and the creation of a Ps Bose–Einstein condensate.

Author Contributions: All authors contributed to all of the material in the manuscript (conceptualization, methodology, investigation, writing and funding acquisition). All authors have read and agreed to the published version of the manuscript.

Funding: This work was supported by Australian Research Council Discovery grant DP200101294 and, in part, by the US National Science Foundation Grant PHY-2110358.

Institutional Review Board Statement: Not applicable.

Informed Consent Statement: Not applicable.

Data Availability Statement: All relevant data is contained in the manuscript.

Conflicts of Interest: The authors declare no conflict of interest.

References

1. Maekawa, M.; Fukaya, Y.; Yabuuchi, A.; Mochizuki, I.; Kawasuso, A. Development of Spin Polarized Slow Positron Beam Using a ^{68}Ge – ^{68}Ga Positron Source. *Nucl. Instrum. Methods Phys. Res. Sect. B Beam Interact. Mater. At.* **2013**, *308*, 9–14. [[CrossRef](#)]
2. Wada, K.; Miyashita, A.; Maekawa, M.; Sakai, S.; Kawasuso, A. Spin Polarized Positron Beams with ^{22}Na and ^{68}Ge and Their Applications to Materials Research. *AIP Conf. Proc.* **2018**, *1970*, 040001.
3. Maekawa, M.; Miyashita, A.; Sakai, S.; Li, S.; Entani, S.; Kawasuso, A. Spin-Polarized Positronium Time-of-Flight Spectroscopy for Probing Spin-Polarized Surface Electronic States. *Phys. Rev. Lett.* **2021**, *126*, 186401. [[CrossRef](#)] [[PubMed](#)]
4. Mills, A.P. Proposal for a Slow Positron Facility at Jefferson Laboratory. *AIP Conf. Proc.* **2018**, *1970*, 040002.
5. Cortese, E.; Cassidy, D.B.; de Liberato, S. Positronium Density Measurements Using Polaritonic Effects. *arXiv* **2022**, arXiv:2210.09875v1. [[CrossRef](#)]
6. Cassidy, D.B.; Mills, A.P. Enhanced Ps-Ps Interactions due to Quantum Confinement. *Phys. Rev. Lett.* **2011**, *107*, 213401. [[CrossRef](#)]
7. Mills, A.P. Possible Experiments with High Density Positronium. *AIP Conf. Proc.* **2019**, *2182*, 030001.
8. Rich, A. Recent Experimental Advances in Positronium Research. *Rev. Mod. Phys.* **1981**, *53*, 127–165. [[CrossRef](#)]
9. Perkins, D.H. *Introduction to High Energy Physics*, 3rd ed.; Addison Wesley: Menlo Park, CA, USA, 1987; Section 7.5.
10. Major, J. *Positron Beams and Their Applications*; Coleman, P.G., Ed.; World Scientific: Singapore, 2000; Chapter 9.
11. Charlton, M.; Humberston, J.W. *Positron Physics*; Cambridge University Press: Cambridge, UK, 2001.
12. Massey, H.S.W. The Elastic Scattering of Fast Positrons by Heavy Nuclei. *Proc. Roy. Soc. A* **1942**, *181*, 14–19.
13. Van Klinken, J.; Venema, W.Z.; Wichers, V.A. A Fourfold Bhabha/Moller Polarimeter for Positrons/Electrons. *Nucl. Instrum. Methods Phys. Res. Sect. A Accel. Spectrometers Detect. Assoc. Equip.* **1990**, *286*, 202–213. [[CrossRef](#)]
14. Charlton, M. Experimental Studies of Positrons Scattering in Gases. *Rep. Prog. Phys.* **1985**, *48*, 737–793. [[CrossRef](#)]
15. Hanna, S.S.; Preston, R.S. Positron Polarization Demonstrated by Annihilation in Magnetized Iron. *Phys. Rev.* **1957**, *106*, 1363–1364. [[CrossRef](#)]
16. Nagashima, Y.; Hyodo, T. Effects of Positron Spin Polarization on Orthopositronium and Parapositronium formation in a magnetic field. *Phys. Rev. B* **1990**, *7*, 3937–3942. [[CrossRef](#)] [[PubMed](#)]
17. Page, L.A.; Heinberg, M. Measurement of the Longitudinal Polarization of Positrons Emitted by Sodium-22. *Phys. Rev.* **1957**, *106*, 1220–1224. [[CrossRef](#)]
18. Telegdi, V.; Grodzins, L. Measurement of Helicity. *Prog. Nucl. Phys.* **1959**, *7*, 165–241.
19. Lundby, A. Weak interactions: Experiments on parity, charge conjugation and time reversal symmetries. *Prog. Elem. Part. Cosm. Ray Phys.* **1960**, *5*, 1–96.
20. Dick, L.; Feuvrais, L.; Madansky, L.; Telegdi, V.L. A Novel Efficient Method for Measuring the Polarization of Positrons. *Phys. Lett.* **1963**, *3*, 326–329. [[CrossRef](#)]
21. Bisi, A.; Fiorentini, A.; Gatti, E.; Zappa, L. Magnetic Quenching of Positronium in Solids and Positron Helicity. *Phys. Rev.* **1962**, *128*, 2195–2199. [[CrossRef](#)]
22. Gerber, G.; Newman, D.; Rich, A.; Sweetman, E. Precision Measurement of Positron Polarization in ^{68}Ga Decay based on the Use of a New Positron Polarimeter. *Phys. Rev. D* **1977**, *15*, 1189–1193. [[CrossRef](#)]
23. Zitzewitz, P.W.; Van House, J.C.; Rich, A.; Gidley, D.W. Spin Polarization of Low Energy Positron Beams. *Phys. Rev. Lett.* **1979**, *43*, 1281–1284. [[CrossRef](#)]
24. Skalsey, M.; Girard, T.A.; Newman, D.; Rich, A. New Method for Precision Polarimetry: First Results and Future Applications. *Phys. Rev. Lett.* **1982**, *49*, 708–711. [[CrossRef](#)]
25. Kumita, T.; Chiba, M.; Hamatsu, R.; Hirose, M.; Hirose, T.; Irako, M.; Kawasaki, N.; Yang, J. Design of a Polarimeter for Slow e^+ Beams. *Nucl. Instrum. Methods Phys. Res. Sect. A Accel. Spectrometers Detect. Assoc. Equip.* **2000**, *440*, 172–180. [[CrossRef](#)]
26. Cassidy, D.B.; Meligne, V.E.; Mills, A.P. Production of a Fully Spin-Polarized Ensemble of Positronium Atoms. *Phys. Rev. Lett.* **2010**, *104*, 173401. [[CrossRef](#)] [[PubMed](#)]

27. Murphy, T.; Surko, C.M. Positron Trapping in an Electrostatic Well by Inelastic Collisions with Nitrogen Molecules. *Phys. Rev. A* **1992**, *46*, 5696–5705. [[CrossRef](#)] [[PubMed](#)]
28. Happer, W. Optical Pumping. *Rev. Mod. Phys.* **1972**, *44*, 169–249. [[CrossRef](#)]
29. Pirbhai, M.; Knepper, J.; Litaker, E.T.; Tupa, D.; Gay, T.J. Optically Pumped Spin-Exchange Polarized Electron Source. *Phys. Rev. A* **2013**, *88*, 60701. [[CrossRef](#)]
30. Tupa, D.; Anderson, L.W.; Huber, D.L.; Lawler, J.E. Effect of Radiation Trapping on the Polarization of an Optically Pumped Alkali-Metal Vapor. *Phys. Rev.* **1986**, *A33*, 1045–1051. [[CrossRef](#)]
31. Tupa, D.; Anderson, L.W. Effect of Radiation Trapping on the Polarization of an Optically Pumped Alkali-Metal Vapor in a Weak Magnetic Field. *Phys. Rev. A* **1987**, *36*, 2142–2147. [[CrossRef](#)]
32. Wu, W.; Kitano, M.; Happer, W.; Hou, M.; Daniels, J. Optical Determination of Alkali Metal Vapor Number Density Using Faraday Rotation. *Appl. Opt.* **1986**, *25*, 4483–4492. [[CrossRef](#)]
33. Young, J.A.; Surko, C.M. Charged Particle Motion in Spatially Varying Electric and Magnetic Fields. *Nucl. Instrum. Methods Phys. Res. Sect. B Beam Interact. Mater. At.* **2006**, *247*, 147–154. [[CrossRef](#)]
34. Greaves, R.G.; Moxom, J.M. Compression of Trapped Positrons in a Single Particle Regime by a Rotating Electric Field. *Phys. Plasmas* **2008**, *15*, 072304. [[CrossRef](#)]
35. Deller, A.; Mortensen, T.; Isaac, C.A.; van der Werf, D.P.; Charlton, M. Radially Selective Inward Transport of Positrons in a Penning-Malmberg Trap. *New J. Phys.* **2014**, *16*, 073028. [[CrossRef](#)]
36. Rosenberry, M.A.; Reyes, J.P.; Tupa, D.; Gay, T.J. Radiation Trapping in Rubidium Optical Pumping at Low Buffer-Gas Pressures. *Phys. Rev. A* **2007**, *75*, 023401. [[CrossRef](#)]
37. Oro, D.M.; Lin, Q.; Soletsky, P.A.; Zhang, X.; Dunning, F.B.; Walters, G.K. Absolute Calibration of a Mott Polarimeter Using Surface Penning Ionization. *Rev. Sci. Instrum.* **1992**, *63*, 3519–3520. [[CrossRef](#)]
38. Roy, D. Characteristics of the Trochoidal Monochromator by Calculation of Electron Energy Distribution. *Rev. Sci. Instrum.* **1972**, *43*, 535–541. [[CrossRef](#)]
39. El-Gamal, H.; Negm, H.; Hasabelnaby, M.J. Detection Efficiency of NaI(Tl) Detector Based on the Fabricated Calibration of HPGe Detector. *Rad. Res. Appl. Sci.* **2019**, *12*, 360–366. [[CrossRef](#)]
40. Machacek, J.R.; McTaggart, S.; Burggraf, L.W. Single-shot positron annihilation lifetime spectroscopy using a liquid scintillator. *AIP Adv.* **2021**, *11*, 055223. [[CrossRef](#)]
41. Alonso, A.M.; Cooper, B.S.; Deller, A.; Cassidy, D.B. Single-shot positron annihilation lifetime spectroscopy with LYSO scintillators. *Nucl. Instrum. Methods Phys. Res. Sect. A Accel. Spectrometers Detect. Assoc. Equip.* **2016**, *828*, 163–169. [[CrossRef](#)]
42. Ratnavelu, K.; Brunger, M.J.; Buckman, S.J. Recommended Positron Scattering Cross Sections for Atomic Systems. *J. Phys. Chem. Ref. Data* **2019**, *48*, 023102. [[CrossRef](#)]
43. Cassidy, D.B. Experimental Progress in Positronium Laser Physics. *Eur. Phys. J. D* **2018**, *72*, 53. [[CrossRef](#)]
44. Kernoghan, A.A.; McAlinden, M.T.; Walters, H.R.J. Positron Scattering by Rubidium and Caesium. *J. Phys. B* **1996**, *29*, 3971–3988. [[CrossRef](#)]
45. Surdutovich, A.; Jiang, J.; Kauppila, W.E.; Kwan, C.K.; Stein, T.S.; Zhou, S. Measurement of Positronium Formation Cross Sections for Positrons Scattered by Rb Atoms. *Phys. Rev. A* **1996**, *53*, 2861–2864. [[CrossRef](#)]
46. Kessler, J. *Polarized Electrons*, 2nd ed.; Springer: Berlin/Heidelberg, Germany, 1986.
47. Ahrendsen, K.J.; Brunner, W.J.; Gay, T.J. Studies of Collision Dynamics in Rb Spin-Exchange Cells. *Bull. Am. Phys. Soc.* **2019**, *64*, E01.00020.
48. Radwell, N.; Walker, G.; Franke-Arnold, S. Cold Atom Densities of More Than 10^{12} cm^{-3} in a Holographically Shaped Dark Spontaneous-Force Optical Trap. *Phys. Rev. A* **2013**, *88*, 043409. [[CrossRef](#)]
49. Dedman, C.J.; Baldwin, K.G.H.; Colla, M. Fast Switching of Magnetic Fields in a Magneto Optic Trap. *Rev. Sci. Instrum.* **2001**, *72*, 4055–4058. [[CrossRef](#)]

Disclaimer/Publisher’s Note: The statements, opinions and data contained in all publications are solely those of the individual author(s) and contributor(s) and not of MDPI and/or the editor(s). MDPI and/or the editor(s) disclaim responsibility for any injury to people or property resulting from any ideas, methods, instructions or products referred to in the content.